Helical channel studies and simulations

V.Balbekov

Fermi National Accelerator Laboratory, Batavia, IL 60510

August 7, 2000

Abstract

Results of studies and simulation of a cooler with helical magnetic field and emittance exchange proposed in [1] are presented. Investigation of transverse and longitudinal nonlinear effects is performed and used for a choice of the cooling channel parameters. The main solenoid of 72 m length has field strength 5 T. Transverse helical field has amplitude 0.3 T and period 1.8 m. A possibility to generate this field by means of an inclination or shift of the solenoid sections is considered. With LiH wedge absorbers the cooler provides decrease of longitudinal emittance by factor 0.87. Transmission reaches 83% being 10% less in comparison with the same channel without emittance exchange. Longitudinal perturbation due to transverse magnetic field is responsible for this degradation. A possibility to weaken this effect by entering of energy-transverse momentum correlation in the beam is discussed.

1 Introduction

Complete linear theory of ionization cooling on spiral orbit is propounded by Y.Derbenev [1]. Several simplified formulae useful for choice of the cooler parameters and simulations are presented in this section.

In laboratory frame, a helical magnetic field has the components:

$$B_x = B_t\left(\sin\frac{2\pi z}{L} + O\left(\frac{r^2}{L^2}\right)\right) \quad (1)$$

$$B_y = B_t\left(\cos\frac{2\pi z}{L} + O\left(\frac{r^2}{L^2}\right)\right) \quad (2)$$

$$B_z = B_0\left(1 + O\left(\frac{B_t r}{B_0 L}\right)\right) \quad (3)$$

where B_0 is the field of main solenoid, B_t is amplitude of transverse dipole field, L is the helix period, and r is a particle radius. In this section we will use paraxial approximation and neglect all the terms like $O(...)$ assuming:

$$\frac{p_t}{p} \ll 1, \quad \frac{r^2}{L^2} \ll 1, \quad \frac{B_t r}{B_0 L} \ll 1, \quad (4)$$

where p and p_t are total and transverse momenta of a particle. All these terms will be taken into account later at the simulations.

In this approximation, equations of motion can be written in the following complex form:

$$\frac{d(x+iy)}{dz} = \frac{\Pi}{p}, \quad (5)$$

$$\frac{d(p_x + ip_y)}{dz} = -i\frac{eB_z}{pc}(p_x + ip_y) - \frac{eB_t}{c}\exp\left(-i\frac{2\pi z}{L}\right), \quad (6)$$

The solution is:

$$x + iy = \left(\frac{L}{2\pi}\right)^2 \frac{eB_t}{c(p - p_{res})}\exp\left(-\frac{2\pi i z}{L}\right) + C_1\exp\left(-i\frac{ieB_0}{pc}\right) + C_2, \quad (7)$$

$$p_x + ip_y = -i\left(\frac{L}{2\pi}\right)\frac{eB_t p}{c(p - p_{res})}\exp\left(-\frac{2\pi i z}{L}\right) - iC_1\frac{eB_0}{c}\exp\left(-i\frac{ieB_0}{pc}\right), \quad (8)$$

where $p_{res} = eB_0L/(2\pi c)$ is the resonance momentum. First term in these expressions is a spiral periodic orbit, second one describes Larmor rotation around it. Constant C_2 reflects an absence of a natural center of the system, because the field does not depend on x and y in given approximation.

The usual dispersion function can be written as

$$\psi_x + i\psi_y = \left(p\frac{d(x+iy)}{dp}\right)_{periodical} = -\left(\frac{L}{2\pi}\right)^2 \frac{eB_t p}{c(p-p_{res})^2}\exp\left(-\frac{2\pi i z}{L}\right) \quad (9)$$

Dependence of x, p_y, and ψ_x on energy is plotted in Fig.1 at $z = nL$ where n is any integer. The following parameters are used:

$$B_0 = 5\ \mathrm{T}, \quad B_t = 0.3\ \mathrm{T}, \quad L = 180\ \mathrm{cm}.$$

(reasons for such a choice are discussed in the next sections). It is seen that the dispersion function of the channel is not large and comparable with periodical orbit deviation. For example, at radius of periodical orbit is 3.8 cm, and $\psi_x = 4.8$ cm at $E_{tot} = 260$ MeV.

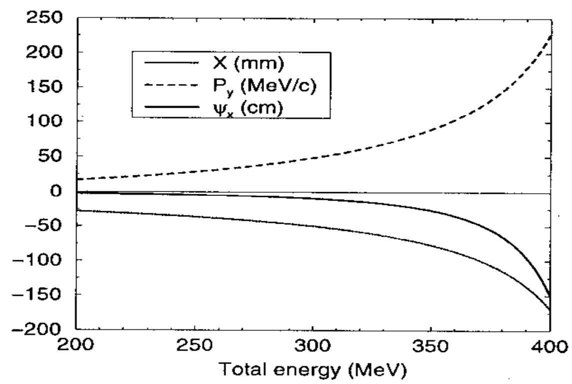

Figure 1: Periodical orbit and dispersion function at $z = nL$.

2 Quasiperiodical orbits in adiabatical field

In any real channel of terminal length there are some exitation of betatron oscillations by dipole field in the beginning and the end of the channel. An adiabatic growth of the dipole field at the beginning and decay at the end is, probably, the simplest way to avoide it. An example is given in Fig.2 where the following dependence of the field amplitude on z is considered:

- Linear growth of B_t from 0 to 0.3 T in first 8 periods (14.4m);
- $B_t = 0.3$ T in next 24 periods (in princilpe, this number is arbitrary);
- Linear decay of the field from 0.3 T to 0 in the latest 8 periods.

Quasiperiodical orbits are shown for three energies corresponding approximately to central, minimal, and maximal energy of particles in the bucket. The central orbit is plotted in detail, and two others with step 180 cm (the field period) that gives their envelops. A modulation of the orbit radius increases when the particle energy approaches to resonanse and becomes considerable at $E > 380$ MeV. It corresponds $p_{max}/p_{res} \simeq 0.85$ that is, probably, maximal allowable ratio. For given case, $p_{res} = 429$ MeV/c corresponding $E_{res} = 442$ MeV. As follows from definition after Eq.(8), $p_{res} \propto L$, i.e. a shortening of the field period is required to decrease it. A creating of a short-period field is a difficult engineering problem discussed in the Appendix. It is a short explanation why the channel parameters as above are chosen. More detailed analysis is given in the next sections.

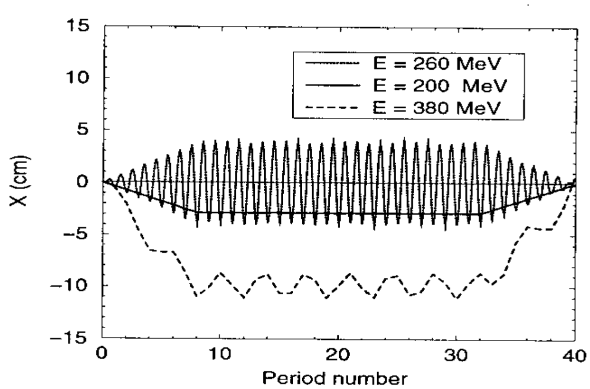

Figure 2: Quaziperiodical orbit in adiabatical dipole magnetic field.

3 Absorbers

The best positions of wedge absorbers are the beginning of the channel and further by step $L/2$. As follows from Eq.(9) and Fig.2, dispersion function has here only X-component $\mp\psi$ here:

$$\psi = -\left(\frac{L}{2\pi}\right)^2 \frac{eB_t p}{c(p_{res} - p)^2} \tag{10}$$

The wedge absorbers should be placed around periodical orbit of the reference particle which is $\mp x_{ref}$ where

$$x_{ref} = \left(\frac{L}{2\pi}\right)^2 \frac{eB_t}{c(p_{res} - p)} \tag{11}$$

Each absorber should provide energy loss

$$\Delta E = \pm\kappa(x - x_{ref}) \tag{12}$$

In this case energy loss per period does not depend on initial transverse coordinate of muon i.e. on constant C_2 in Eq.7. Designating energy of a particle as $E = E_{ref} + W$ one can get the following expression for relative decrease of energy spread by single wedge absorber:

$$\frac{\Delta W}{W} = -\frac{\kappa(x - x_{ref})}{W} = -\kappa\psi\frac{\Delta p}{pW} = -\frac{\kappa\psi}{\beta^2 E_{ref}} \tag{13}$$

We assume that average accelerating gradient $V' = 14$ MV/m, and synchronous phase $\phi_{syn} = 30^o$. Then energy gain per half-period as 7 MeV/m$\times$ 0.9 m = 6.3 MeV. Estimated half-width of the beam is about 15 cm, i.e. strength of the wedge absorber cannot exceed 6.3 MeV/15 cm = 0.42 MeV/cm. At $\psi = 4.8$ cm, and $E_{ref} = 260$ MeV it gives very modest damping $\Delta W/W \simeq -0.009$ which is only slightly more than 'natural' growth due to dependence of energy loss on energy. It means that only wedge absorbers can be used in such a channel. Liquid hydrogen is probably not suitable for this. Therefore lithium hydride absorbers are considered below with the following sizes: width 30 cm, thickness 3.88 cm at center.

4 Nonlinear effects

Cooling channel 72 m long (40 cells), with dipole field and absorbers described above is considered in this section. 201 MHz cavities placed between absorbers provide average accelerating gradient 14 MeV/m at synchronous phase 30^o. All the nonlinearities are taken into account at the tracking. Scattering and straggling in absorbers are not considered in this section.

Fig.3 (left) represents X-trajectory and energy of the particle at initial conditions:

$$x = y = p_x = p_y = 0, \quad \phi = \phi_{syn} = 30^o, \quad E = E_{ref} = 260 \text{ MeV}.$$

Arising acceleration and synchrotron oscillations mean that it is non-equilibrium particle. The explanation is an excitation of transverse momentum by dipole field with corresponding decrease of longitudinal velocity. It is necessary to accommodate the reference energy to transverse momentum of the particle on equilibrium orbit to suppress this effect:

$$E_{ref} = \frac{E_0}{\sqrt{1 + (p_t/mc)^2}}, \tag{14}$$

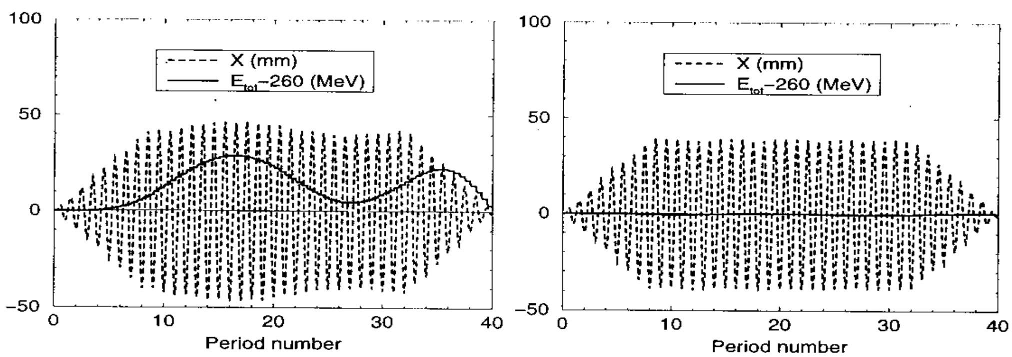

Figure 3: Dependence of X and E on distance for equilibrium particle (left: E_{ref} = 260 MeV; right: E_{ref} is determined by Eq.(13).

where $p_t = \sqrt{p_x^2 + p_y^2}$ is determined by Eq.(5) at $C_1 = 0$. The result is represented in Fig.3 (right) and shows that this particle becomes equilibrium.

Because of the dependence of longitudinal velocity on transverse momentum, a topology of longitudinal phase space is rather unusual. It is illustrated by Fig.4 (left) where several phase trajectories projected on energy-time plane are shown at $E_0 = 260$ MeV and initial conditions $x = y = p_x = p_y = 0$ (the channel is lengthened up to 144 m in this case to increase number of betatron oscillations and to get more informative pictures). First of all stands out second region of stability B. It has the following explanation: transverse momentum of particles growths so fast near the resonance that longitudinal velocity decreases when energy increases. As a result, the velocity is approximately the same at $E_{tot} = 260$ MeV (center of main region of stability A), and $E_{tot} \simeq 400$ MeV, resulting an appearance of the second stable point. It exists only due to dipole field and disappears after it is turned off resulting an unstable moving along line *bb*.

Maybe this effect can be used for storage of muons in this additional buckets. However dynamics of this storage is very complicated and does not considered in this paper. On the contrary, maintenance of main stability region A is treated here as a key point. A superfluous approach to the

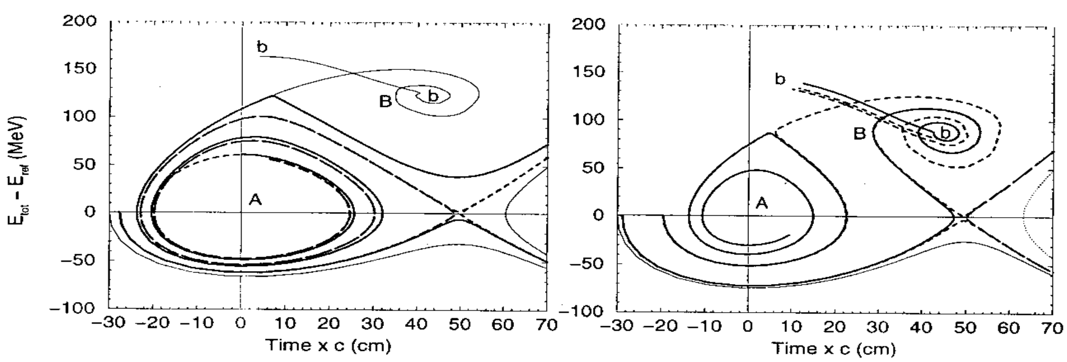

Figure 4: Longitudinal phase space at $E_0 = 260$ MeV (left) and $E_0 = 280$ MeV (right).

resonance is most dangerous from this point of view. It is illustrated by Fig.4 (right) where longitudinal phase space is shown at $E_0 = 280$ MeV. It is seen that area of the bucket A is reduced here by factor about 2. A moving off from the resonance results more traditional shape of the bucket but decreases longitudinal decrement because of decrease of dispersion. For given case, the 'threshold' energy is 234 MeV when the decrement is about 0. Therefore energy $E_0 = 260$ MeV is chosen as an optimal for this channel.

Trajectories of several particles on x vs z are shown in Fig.5 at initial conditions: $E_{tot} = E_0 = 260$ MeV, $\phi = 30^o$, $y = p_x = p_y = 0$, and different x. It should be no dependence on x_{in} in approximation (4); however real (nonlinear) field has a center resulting slow oscillating term instead of C_2 in Eq.(7). These oscillations do not attenuate at ionization cooling. And what is more, their amplitude slowly growths because of synchro-betatron resonance caused by high frequency modulation of energy loss in absorbers which are

$$\Delta E = \Delta E_{ave} \pm \kappa x_{in}$$

(see Eq.(12)). It is illustrated by Fig.5 (right) where the same effect is considered at linear magnetic field i.e. in apx.(4). As a whole, this effect is very slow and not dangerous in practice.

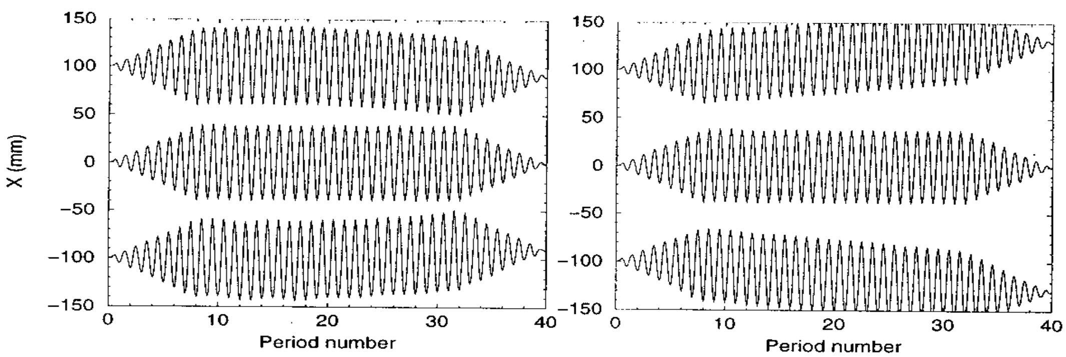

Figure 5: Dependence of x on distance at nonlinear (left) and linear (right) magnetic field.

Trajectories of several particles (r vs z) with non-zero initial transverse momentum are plotted in Fig.6 at the same initial energy and phase, and $x_{in} = 0$. Oscillations of radius are free betatron oscillations which attenuate due to cooling (left plot). Arising synchrotron oscillations attenuate also due to emittance exchange until they are enough small. However increase of transverse momentum makes worse the longitudinal stability. As follows from Fig.5 (right), maximal allowable transverse momentum is 76 MeV/c, after that the particle is captured in region B. It is only about 1.5σ for a realistic beam that is not enough for the cooling and requires an improvement.

The origin of this effect is the same as the energy modulation in Fig.3, that is a dependence of longitudinal velocity on transverse momentum. Therefore E-p_t - correlation in the initial distribution like described by Eq.(14) should improve the situation:

$$E = E_0\sqrt{1 + \left(\frac{p_t}{mc}\right)^2} + \Delta E, \tag{15}$$

where p_x, p_y, and ΔE are normal random values. Probably, such a correlation should arise at a bunching of the beam before the cooling. At least it had been observed at the simulation of pre-cooling part and single field flip channel [2]. Of course, it should be checked for helical channel, too, however it is a

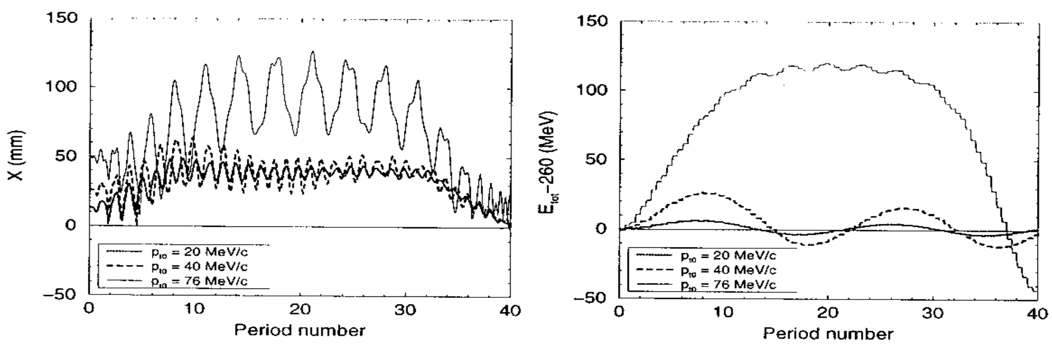

Figure 6: Dependence of x and $E - tot$ on distance for particles with non-equilibrium initial transverse momentum without E-p_t - correlation.

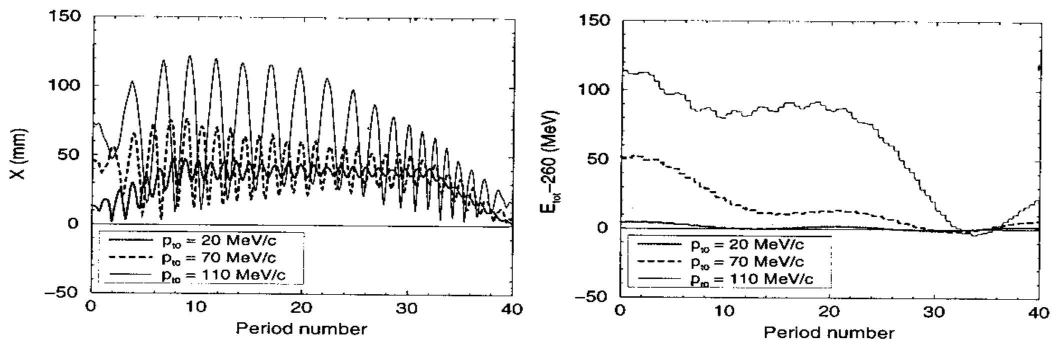

Figure 7: Dependence of x and $E - tot$ on distance for particles with non-equilibrium initial transverse momentum with E-p_t - correlation.

subject of a further investigation. In this paper we will assume that such a correlation is possible in practice. Corresponding trajectories are plotted in Fig.7. Damping of betatron oscillations looks very nice in this case (left plot), and allowable transverse momentum is about 110 MeV/c (right). At this condition, the particle energy tends to equilibrium without large synchrotron oscillations simply because of decrease of transverse momentum.

5 The cooling simulation

All things considered, the following parameters are taken for simulations:

- The channel length: 40 cells $\times$ 1.8 m = 72 m.
- Main solenoid: field 5 T, windows $R = 25$ cm.
- Dipole field: maximal 0.3 T, linear growth/decay by 14.4 m at the beginning and the end of the cooler.
- Wedge absorbers: LiH, width 30 cm, thickness in center 3.88 cm, space 0.9 m, horizontal position is described by Eq.(11), angle is directed to the solenoid axis.
- RF-system: frequency 201 MHz, 3 cavities between absorbers, 4.2 MV each, synchronous phase 30^o.

Initial beam has Gaussian distribution of Larmor centers and transverse momenta with dispersions:

$$\sigma_{Lx} = \sigma_{Ly} = 3.25 \text{ cm}; \quad \sigma_{px} = \sigma_{py} = 48.7 \text{ MeV/c}.$$

Position of Larmor center is determined as

$$x_L = x + \frac{cp_y}{eB_0}, \quad y_L = y - \frac{cp_x}{eB_0}$$

Given ratio σ_p/σ_L corresponds to zero canonical angular momentum of the beam. Longitudinal distribution is Gaussian also with central energy $E_{tot} =$ 260 MeV and dispersions:

$$\sigma_E = 25 \text{ MeV}; \quad \sigma_\tau = 10 \text{ cm}.$$

where $\tau = ct$. If needed, E-p_t - correlation is incorporated additionally by Eq.(15). In any case the reference energy was determined by Eq.(14).

These initial beam parameters as well as parameters of the cooled beam are given *inside* the solenoid. It means that strong x-p_y and y-p_x correlation (i.e. non-zero angular momentum) can arise after the exit from the solenoid. As usually, a field flip and subsequent cooling in a solenoid with opposite magnetic field are needed to suppress it. This part is presumed but not considered in this paper.

Results of the simulation are presented in Figs.8 and Table 1. Five simulations with 10000 particles was performed:

1. Paraxial approximation: magnetic field if the form (1)-(3) at assumptions (4). Evolution of the beam emittance and transmission are presented in left upper plot by thin lines. Total particles loss is 7% in this case, 4.5% of them due to decay. Longitudinal emittance decreases on 18% due to emittance exchange.

2. Nonlinear consideration with the only exception: dependence of longitudinal velocity on transverse momentum is not taken into account i.e. $v_z = v$ is assumed. The results are very close to previous and are plotted on the same figure by bold lines. The transmission is less on 1%, transverse emittance is more on 9%, longitudinal emittance is about the same. It means in particular that nonlinear additions to the magnetic field are not very important.

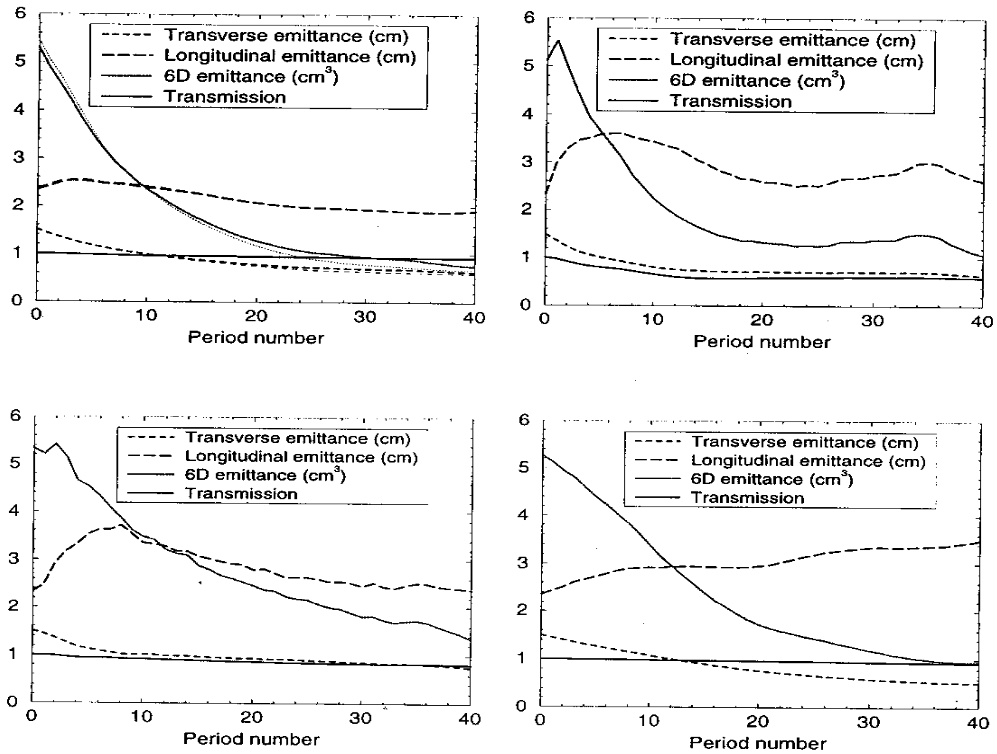

Figure 8: Cooling at 72 m long channel. Left up: linear approximation (thin lines) and with transverse nonlinearity (bold). Right up: all the nonlinearities are taken into account. Left down: with energy - transverse momentum correlations. Right down: without emittance exchange.

3. Totally nonlinear consideration including longitudinal motion. The results plotted in right upper Fig.8 look essentially worse. There is significant longitudinal blow up in the 1st part of the channel. Subsequent decrease of the emittance is explained mainly by the particles loss which is about 40%. Of course, a cooler with similar characteristics is unacceptable in practice.

4. Correlation (15) was used in initial distribution to resolve this problem. The results presented in Fig.8 (left down) look much better. The transmission is 83%, and longitudinal emittance is approximately the same as in case 2. Some increase of transverse emittance is explained, probably, by the approaching of many particles to the resonance because of more energy resulting a deterioration of the adiabaticity.

5. The same channel without the emittance exchange (no dipole field and wedges) is considered for a comparison (Fig.8 right down). It provides 10% more transmission and 30% less 6D emittance. However phase density in longitudinal phase space is increased in case 4 approximately on 40%.

Table 1: Parameters of cooled beam in different approximations.

	Transverse emit. (cm)	Longitudinal emit. (cm)	6D emit.(cm^3)	Transmission
Linear approximation	0.59	1.9	0.67	0.92
Trans. nonlinearities	0.63	1.9	0.75	0.93
All nonlinearities	0.64	2.6	1.07	0.60
With $E - p_t$-correlation	0.75	2.4	1.35	0.81
Without emittance exchange	0.52	3.5	0.95	0.92

6 Appendix. Helical channel with tilted solenoids

Helical magnetic field can be created by means of tilted solenoids. Possible scheme of the cell is represented in Fig.9 (left). Sections of the solenoid 25 cm long are arranged with interval 45 cm and tilted on ± 0.2 rad in plane yz orxz. Magnetic field on the axis is plotted in Fig.9 (right). It is calculated in thin coil approximation at current density 71.7 kA/cm. Average longitudinal field is 5 T with a negligible modulation. Transverse field is very close to sinusoidal and has amplitude 0.3 T. Probably, it is maximal achievable field because of overlapping of the coils.

Similar result one can obtain using shift of neighboring sections in x and y - directions because transverse dipole field arises between such sections. However the channel aperture decreases in this case more because required shift is about $\pm$ 19 cm.

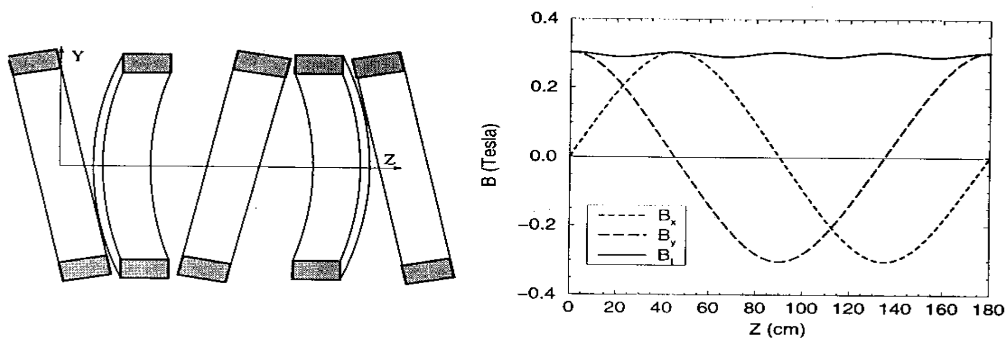

Figure 9: Channel with tilted solenoids: left – schematic, right – magnetic field on the axis.

7 Conclusion

It is shown that emittance exchange is helical magnetic field is really possible, though achievable longitudinal decrement is not large – about 2×10^{-3}/m. Adiabatical growth/decay of dipole magnetic field allows to avoid blow up of transverse emittance in the beginning and the end of the channel. Indispensable condition to avoid longitudinal emittance blow up is energy - transverse momentum correlation of injected beam. At such conditions, transmission 83% is achievable that is 10% less then transmission of similar channel without emittance exchange. 6D phase density goes down due to emittance exchange by factor 0.63 but phase density in longitudinal space increases by factor 1.4. Longitudinal perturbation due to dependence of longitudinal velocity on transverse momentum is the main reason of this degradation.

One of the problems is small dispersion function, what requires as strong wedge absorbers as possible. As a result, usual (not wedge) liquid hydrogen absorbers should be excluded at all. Another demerit is comparatively high energy of cooled beam that decreases cooling factor. However dispersion and efficiency of the emittance exchange go down at lower energy. More dipole field is desirable in this sense; but it creates both engineering and theoretical problems because of stronger longitudinal perturbation.

References

[1] Y.Derbenev, MUCOOL note 134, June 2000.

[2] V.Balbekov, P.Lebrun, J.Monroe, and P.Spentzouris, MUCOOL note 125, May 2000.

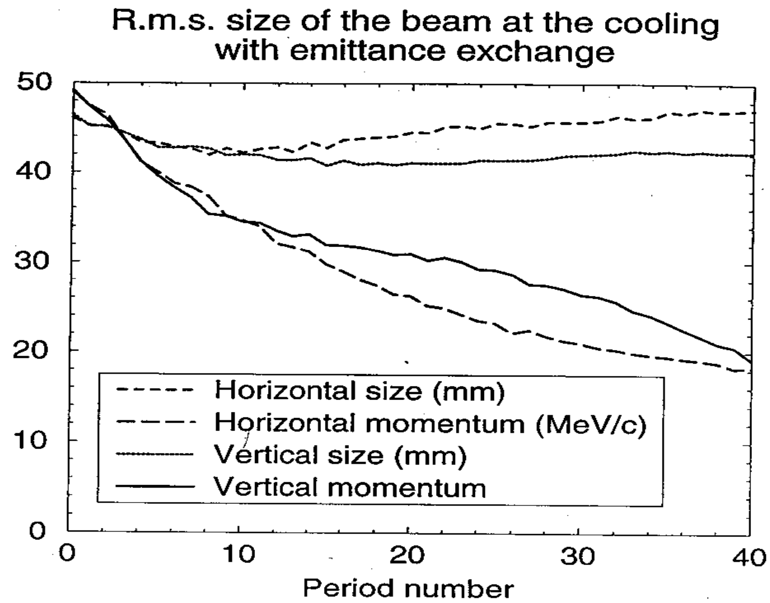
R.m.s. size of the beam at the cooling
with emittance exchange
50
40
30
20
10
0
0
10
20
30
40
Period number
Horizontal size (mm)
Horizontal momentum (MeV/c)
Vertical size (mm)
Vertical momentum

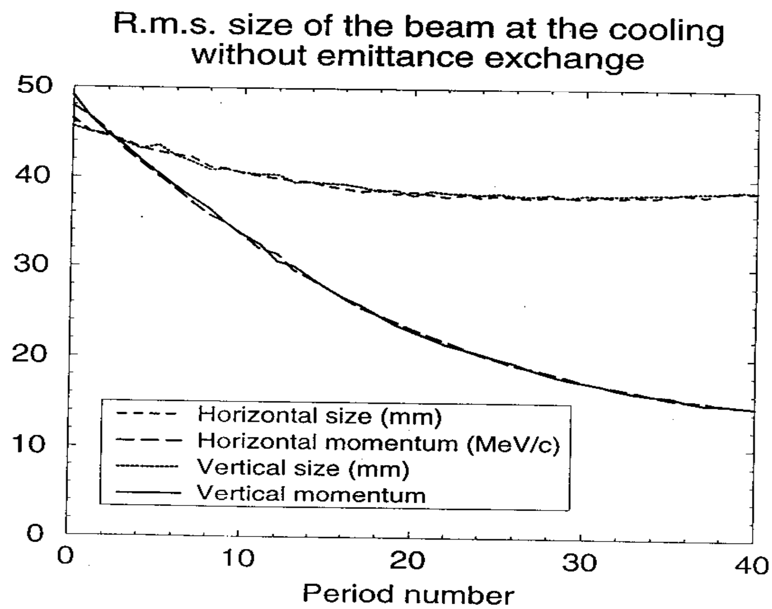
R.m.s. size of the beam at the cooling
without emittance exchange
50
40
30
20
10
0
0
10
20
30
40
Period number
Horizontal size (mm)
Horizontal momentum (MeV/c)
Vertical size (mm)
Vertical momentum

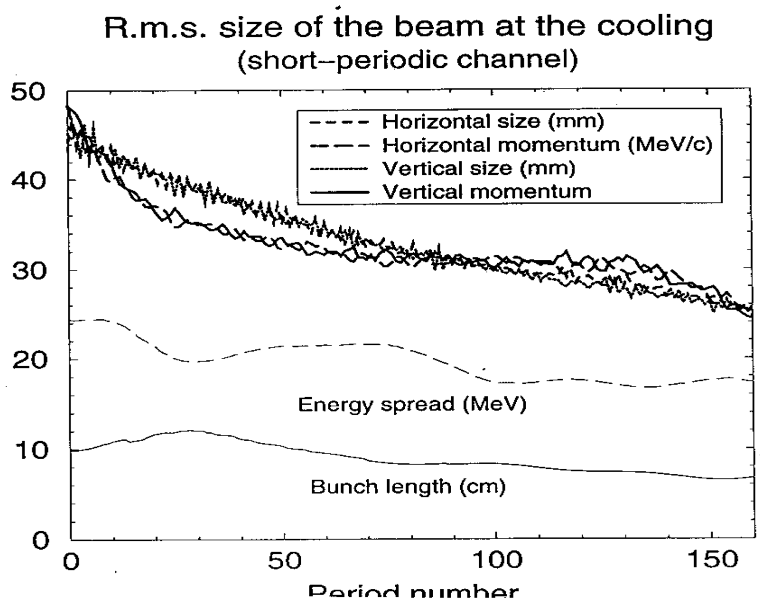
R.m.s. size of the beam at the cooling
(short–periodic channel)
Horizontal size (mm)
Horizontal momentum (MeV/c)
Vertical size (mm)
Vertical momentum
Energy spread (MeV)
Bunch length (cm)
0
10
20
30
40
50
0
50
100
150
Period number

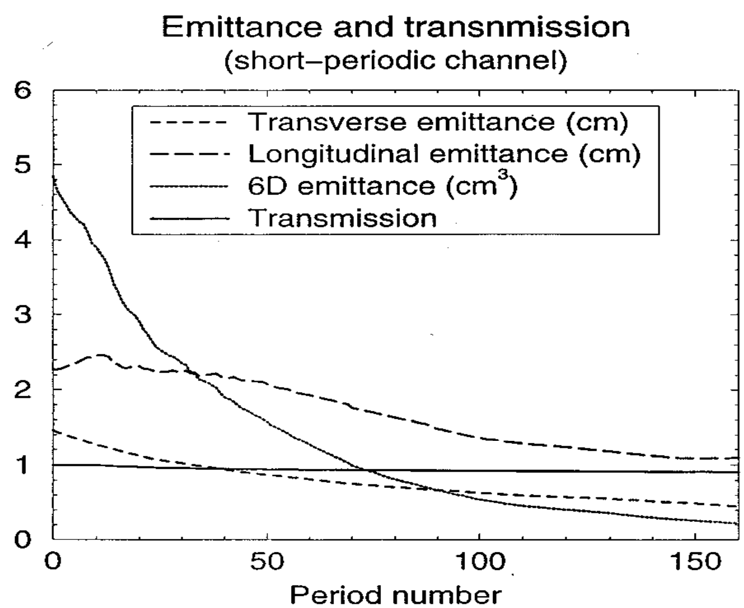
Emittance and transnmission
(short–periodic channel)
Transverse emittance (cm)
Longitudinal emittance (cm)
6D emittance (cm³)
Transmission
0
1
2
3
4
5
6
0
50
100
150
Period number

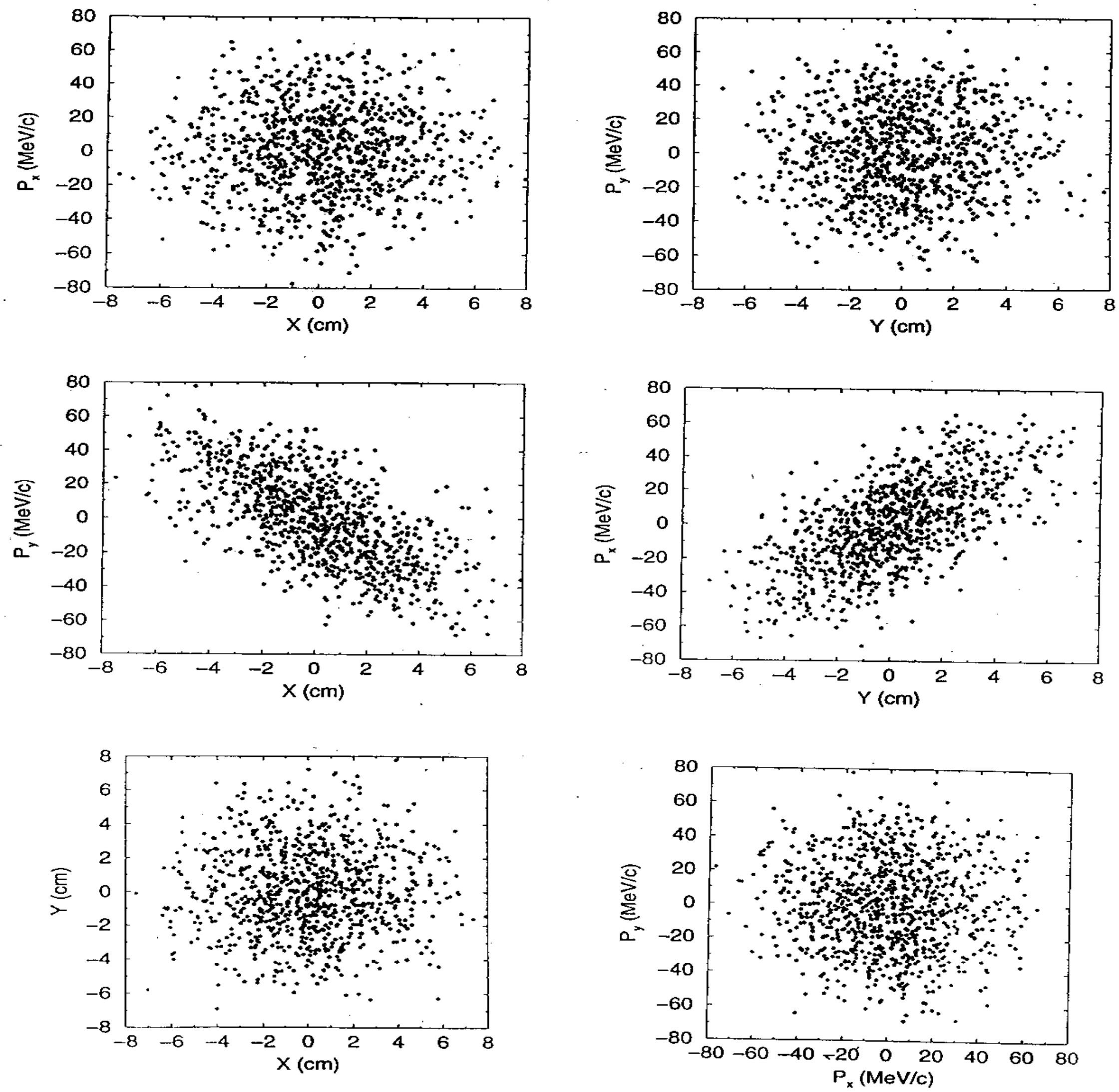

P_x (MeV/c)
X (cm)
P_y (MeV/c)
Y (cm)
P_y (MeV/c)
X (cm)
P_x (MeV/c)
Y (cm)
Y (cm)
X (cm)
P_y (MeV/c)
P_x (MeV/c)